

# On the Relationship between Signal Bandwidth and Frequency Correlation for Surface Forward Scattered Signals

Lee Culver and David Bradley

*Applied Research Laboratory and Graduate Program in Acoustics  
The Pennsylvania State University, P.O. Box 30, State College, PA 16804*

**Abstract.** The relationship between the signal bandwidth and the correlation of a single surface reflected arrival with the transmitted signal has been investigated experimentally and compared with two theories. The dependence of correlation on signal bandwidth is termed *frequency correlation*. Decorrelation of surface scattered signals is a direct consequence of time spread. Thus the acoustic measurement utilized two pure tone signals, from which time spread has been estimated, and four broadband signals with different bandwidths, from which correlation with the transmitted signal has been calculated. A model developed by Dahl for the ocean surface bistatic scattering cross section was used to predict time spread, which agreed very well with the measured time spread. Next, scattering cross section prediction was employed in two theories that predict frequency correlation. The first, published by Reeves in 1974, compared well with the measurements for bandwidths up to 2 kHz, but under predicted correlation for signal bandwidth between 7 and 22 kHz. In the second, linear systems theory was used to develop a mathematical relationship between time spread and frequency correlation. Predictions made using the linear systems theory agree well with the measured values for signal bandwidths up to 22kHz. Further work is required to evaluate the linear systems theory under higher sea state conditions.

## INTRODUCTION

There has been widespread effort in recent years to increase the bandwidth of sonar systems and components (e.g. transducers) in an effort to improve system performance against noise or interference. A relevant question, therefore, is “How much bandwidth will an ocean acoustic channel accommodate without introducing frequency-dependent effects that will degrade coherent processing?” This paper addresses that question for the ocean surface forward scattered acoustic path, and thus applies to signals that have been forward scattered at the ocean surface.

There are many aspects of ocean surface scattering to investigate, understand and model. Fortuin [1] and Ogilvy [2] provide good overviews of ocean surface scattering research. Early efforts were to understand how the mean forward scattered energy varied with sea state, grazing angle, and frequency. More recently, significant progress has been made toward understanding the variation in signal structure caused by changes in transmitter or receiver location, called *spatial coherence*, to understand the limits of acoustic array performance [3]. The focus of the present research is on how the structure of the forward scattered signal is affected by signal bandwidth,

which will be referred to as the *frequency correlation*, in order to determine the limits of broadband sonar performance.

The terms *correlation* and *coherence* can take on different meanings, and so for clarity we now state what we mean by these terms. Consistent with Bendat and Piersol [4], the term *correlation* in this paper refers to the operation

$$\Phi(l, b) = \left\langle \int p_b(t+l) q_b^*(t) dt \right\rangle \quad (1)$$

where  $p_b(t)$  is the received signal with bandwidth  $B$ , and  $q_b(t)$  is a replica of the transmitted signal. Here  $t$  is time,  $l$  is the time lag between  $p_b(t)$  and  $q_b(t)$ , and the brackets  $\langle \rangle$  indicate ensemble averaging.

The term *correlation coefficient* will refer to the normalized correlation:

$$r(l, b) = \left\langle \frac{\int p_b(t) q_b^*(t+l) dt}{\left[ \int |p_b(t)|^2 dt \right]^{1/2} \left[ \int |q_b(t)|^2 dt \right]^{1/2}} \right\rangle \quad (2)$$

which must be between  $-1$  and  $1$ . The term *frequency correlation coefficient* will refer to the dependence of  $r(l, b)$  signal bandwidth  $b$ .

## THEORY PREDICTING FREQUENCY CORRELATION

In 1974, Jon Reeves published theory and measurements that related the decorrelation of a single ocean surface forward scattered arrival to the bandwidth of the signal [5]. That theory was based upon the *time spread*, which is the spreading in time of an acoustic signal due to scattering from bubbles and multiple facets at the ocean boundary. Drawing upon earlier work by Martin [6] and Weston [7], Reeves related frequency correlation to the number of sea surface facets,  $N$ , expected to contribute to the received signal within an interval corresponding to the temporal resolution of the signal. The total of all contributions,  $N_T$ , is proportional to the total temporal elongation (time spread) of the received signal. The number of contributions that are correlated for a particular signal is proportional to the signal time resolution or inverse bandwidth  $\beta^{-1}$ . The correlation estimate is taken as the ratio of the average contributions  $N/N_T$ . The theory thus predicts that increasing bandwidth (meaning increased temporal resolution and thus smaller  $N$ ) results in decreased correlation. Reeves' theory was shown to agree well with correlation measurements using signal bandwidths up to 2 kHz [5].

Dahl [8-10] has developed a detailed model for the bistatic scattering cross section of the ocean surface. The model can be used to compute the intensity impulse response function  $I_{imp}(t)$ , a function which, when convolved with the magnitude squared transmit pulse, produces the ensemble-averaged intensity of a pulse that has been forward scattered from the sea surface. This quantity is known as the time spread. Dahl defines a *characteristic time spread* for the sea-surface bounce path

$$L = \frac{\left[ \int_0^{\infty} I_{imp}(t) dt \right]^2}{\int_0^{\infty} I_{imp}^2(t) dt} \quad \text{sec} \quad (3)$$

and postulates that the inverse of the characteristic time spread,  $L^{-1}$ , with units cycles/sec (Hz), is the channel *frequency coherence bandwidth*, the bandwidth over which coherent processing can be expected to increase the signal to noise ratio.

Ziomek [11] utilizes linear systems theory to define the *transfer function correlation function*

$$R_H(\Delta f, \Delta t) = E \left[ H(f, t) H^*(f + \Delta f, t + \Delta t) \right], \quad (4)$$

which parameterizes how the channel decorrelates the envelopes of different frequency signals, or, more simply, how differently the channel affects signals separated in time  $\Delta t$  and/or frequency  $\Delta f$ . It is the width of  $R_H(\Delta f, \Delta t)$  in frequency that determines the channel frequency correlation. If  $R_H(\Delta f, \Delta t)$  is broad in  $\Delta f$ , broadband signals will suffer minimal decorrelation; if  $R_H(\Delta f, \Delta t)$  is narrow in  $\Delta f$ , correlation will drop off rapidly as signal bandwidth is increased.

Linear systems theory provides a mathematical relationship between the time spread introduced by a channel, e.g. an ocean surface reflection, and the channel transfer function correlation function. The main equations are now reviewed.

Given a source and receiver, the transmitted signal  $x(t)$  and the received signal  $y(t)$  are related through convolution with the linear time varying channel *impulse response function*  $h(t, t)$ :

$$y(t) = \int x(t-t) h(t, t) dt. \quad (5)$$

Here the source directionality and receiver spatial response have been absorbed into  $h(t, t)$ . If the scattering process is wide sense stationary<sup>1</sup> and uncorrelated for different delays, a condition referred to as the *wide-sense stationary uncorrelated scattering (WSSUS)* assumption [11], then the mean square received signal can be expressed as

$$E \left[ |y(t)|^2 \right] = \iint |x(t-t)|^2 R_s(t, f) df dt. \quad (6)$$

Here  $R_s(t, f)$  is the *scattering function*, which parameterizes how the channel spreads acoustic energy in time and frequency. Considering the definition of the intensity impulse response function,  $I_{imp}(t)$ , given above, Equation (6) means that

$$I_{imp}(t) = \int R_s(t, f) df. \quad (7)$$

Now, using the transmitted signal as the replica in Equation (1) defines the *replica correlation function* (for zero Doppler shift or time compression):

$$RC(l, b) = \left\langle \iiint H(f, t) X_b(f) X_b^*(g) \exp(j2pft) \exp(-j2pg(t+l)) df dg dt \right\rangle. \quad (8)$$

<sup>1</sup> The mean and autocorrelation function of a wide sense stationary process do not vary with time [4].

Here  $X_b(f)$  is the Fourier transform of the signal with bandwidth  $b$  and  $H(f, t)$  is the channel transfer function. Under the WSSUS assumption, the mean square replica correlator output can be expressed as

$$E[RC(l, b)^2] = \left\langle \iiint R_H(\Delta f, \Delta t) |\Gamma_b(\Delta f, \Delta t)|^2 \exp(j2p \Delta f l) \Delta f \Delta t \right\rangle \quad (9)$$

where  $\Delta f$  and  $\Delta t$  are frequency and time separations, respectively,  $R_H(\Delta f, \Delta t)$  was defined in Equation (4), and we have introduced a *spectral ambiguity function*

$$\Gamma_b(\Delta f, \Delta t) \equiv \int X_b(f) X_b^*(f + \Delta f) \exp(-j2p f \Delta t) df. \quad (10)$$

Equation (9) provides a method for predicting the mean square replica correlator output for signals with different bandwidths. The spectral ambiguity function of each signal is calculated using Equation (10). From linear system theory, if the WSSUS assumption is valid,  $R_H(\Delta f, \Delta t)$  can be calculated from the scattering function by Fourier transform

$$R_H(\Delta f, \Delta t) = \iint R_S(t, f) \exp(j2p(f\Delta t - \Delta f t)) dt df. \quad (11)$$

If we assume that  $R_S(t, f)$  is separable in  $f$  and  $t$ , then Equation (11) can be integrated over  $f$  and, using Equation (7),

$$R_H(\Delta f, \Delta t) \approx \int I_{imp}(t) \exp(j2p(\Delta f t)) dt. \quad (12)$$

Notice that Equation (9) amounts to multiplying the square of the spectral ambiguity function times the channel transfer function correlation function and integrating over all  $\Delta f$ . Assuming that the functions  $|\Gamma_b(\Delta f, \Delta t)|^2$  are normalized to the same total energy, the replica correlator output will be approximately constant as long as  $|\Gamma_b(\Delta f, \Delta t)|^2$  is narrower than  $R_H(\Delta f, \Delta t)$ . However, once the width of  $|\Gamma_b(\Delta f, \Delta t)|^2$  exceeds that of  $R_H(\Delta f, \Delta t)$ , the replica correlator output will begin to fall off because the signal bandwidth is wider than the channel bandwidth. This is a key explanation for the linear systems theory based predictions.

## TIME SPREAD AND FREQUENCY CORRELATION MEASUREMENTS

Concurrent measurements of time spread and frequency correlation are now described and compared with the theory presented above. An ocean acoustic measurement conducted in August 2002 had, as a primary objective, to directly measure the decorrelation, with increasing signal bandwidth, of direct path, surface reflected, and fully refracted propagation paths through the ocean. Concurrently, ocean surface wave height directional spectra, wind speed and direction, ocean current, and sound speed vs depth were measured in order to investigate the physical mechanisms associated with signal decorrelation. The experiment location was (32° 38.2' N, 117° 57.4' W), which is about 2.5 km east of San Clemente Island and about 80 km west of San Diego, California. Water depth is approximately 500 m.

## Acoustic Measurement Instrumentation

The measurement geometry is shown in Fig. 1. Signals were transmitted from International Transducer Corporation (ITC) 1001 and 6084 acoustic projectors attached to the riser of a bottom-moored surface buoy. The buoy mooring included an elastic section composed of eight 20 m (unstretched) bungee cords capable of being stretched to 60 m, which served to reduce the buoy watch circle to a few 10's of meters. Signals were received at ITC 6080C hydrophones suspended from the research vessel Acoustic Explorer, that ship being in a three-point moor. Elastic tethers were used to decouple the hydrophones from ship heave.

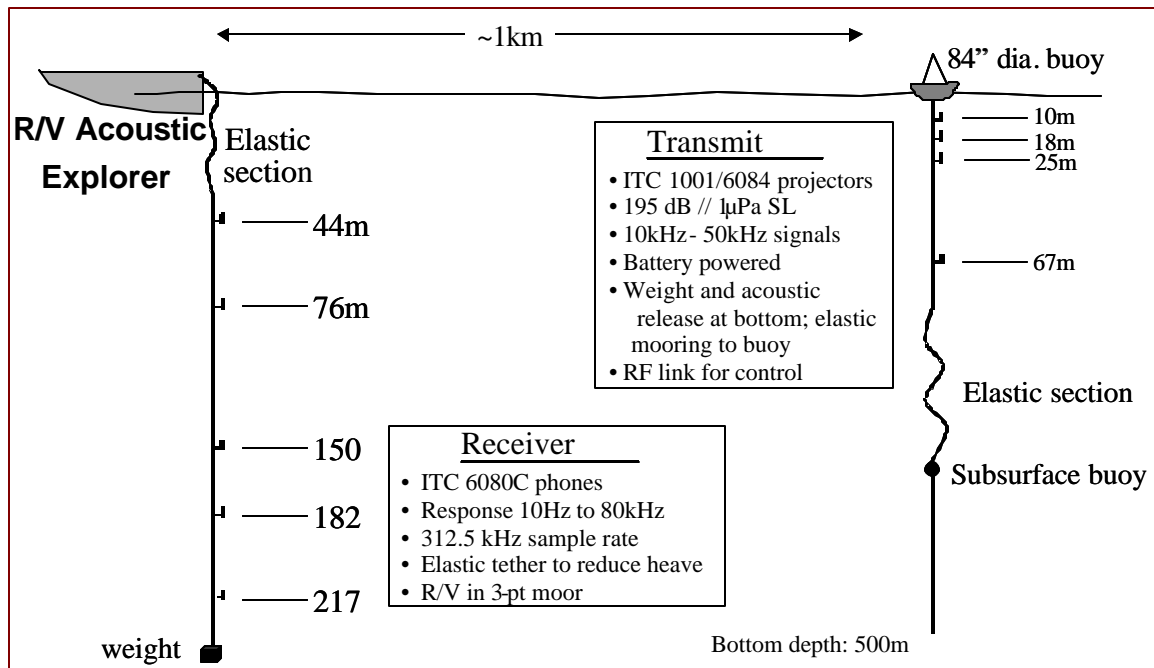


**FIGURE 1.** Measurement geometry , August 2002 about 2.5 km east of San Clemente Is., California.

Transmit electronics were housed in the surface buoy. A compact PCI based computer was controlled via 900 MHz and 2.4 GHz radio frequency (RF) links with the Acoustic Explorer. Twenty-six 12-volt gel cell marine batteries provided power for several days of continuous operation. Signals were clocked out at 125k samples/sec using a CPCI board designed and built by ARL/PSU. An Instruments Inc. L6 amplifier modified by the manufacturer to accept 48 VDC input power was controlled using the remote interface. Only one projector was active at a time, with projector selection accomplished using high current relays. On board the Acoustic Explorer, received signals were bandpass filtered and sampled at 312.5k samples/sec using boards designed and built at ARL/PSU.

## Environmental Measurements

Figure 2 shows a sound speed profile calculated from a CTD drop made during the experiment. It shows a very shallow mixed layer and a strong downward refracting region down to about 100 m, and below that the water is relatively isothermal. A ray-trace made using the Comprehensive Acoustic System Simulation / Gaussian Ray Bundle (CASS/GRAB) acoustic propagation model [12] for the 67 m deep projector and 217 m deep receiver shows slightly refracted direct and a surface reflected paths. For this projector-hydrophone pair, the difference in travel time between the direct and surface reflected paths is about 19 msec.

The measurement site was very much in the lee of San Clemente Island, which significantly affected wind speed and direction and reduced surface wave height. The wind measured at the site of the experiment was from the north-northwest during most of the experiment, and averaged 4 – 6 m/s, corresponding to a sea state 3 on the World Meteorological Organization (WMO) chart [13]. However, a NOAA buoy west of San Clemente Island measured winds from the west, indicating that San Clemente Is. was significantly affecting the wind at the experiment site.

Directional wave height spectra were measured during the experiment using an AXYS Technologies Triaxys wave buoy. A surface waveheight wavenumber spectrum is required as the environmental input to Dahl's bistatic scattering cross section model. For forward scattering geometries, the waveheight spectrum must extend to ocean surface wave numbers of about  $k/4$ , where  $k$  is the acoustic wave number [10]. Using the method developed by Dahl [9], and the "D" wave height spectrum model developed by Plant [14], which uses the wind speed and fetch as inputs, the measured waveheight spectrum was extended to frequencies well above those measured by the wave rider buoy.

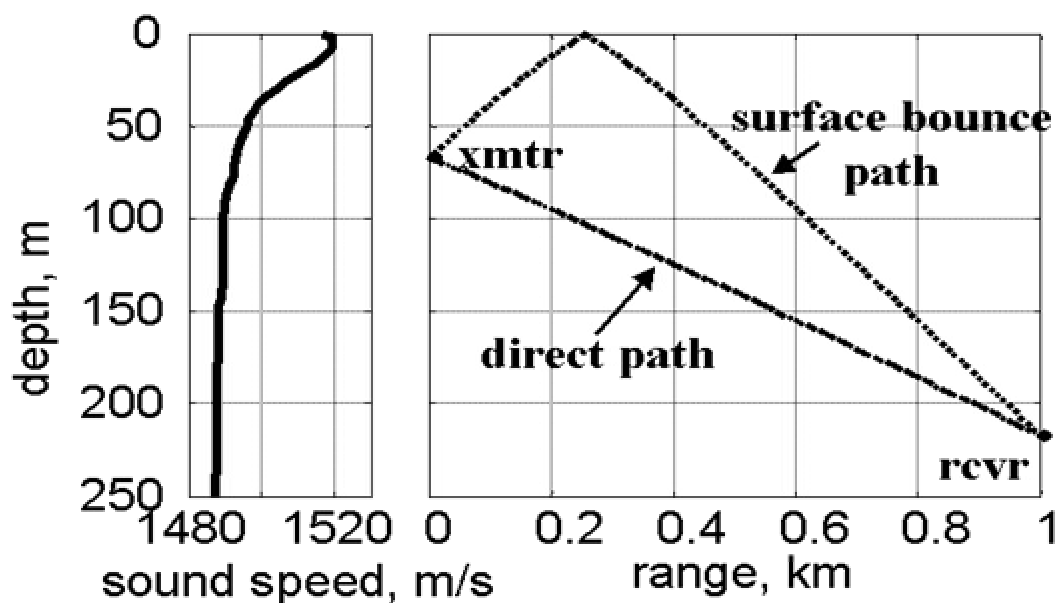


FIGURE 2. Sound speed profile and ray trace between the 67 m deep projector and 217 m deep hydrophone.

## Acoustic Measurements

Moving on now to the acoustic data, the transmit signals are summarized in Table 1. Two Continuous Wave (CW) pulses and four Linear Frequency Modulated (LFM) pulses were transmitted at two different center frequencies. We take the separation between sinc function zero crossings ( $2/T$ ) as the bandwidth of a CW pulse in Table 1.

**TABLE 1.** Signals transmitted at center frequencies of 20kHz and 40kHz

Signal type	Duration	Bandwidth
CW pulse	0.25 ms	8.0 kHz
CW pulse	1.0 ms	2.0 kHz
LFM	8.0 ms *	1.0 kHz
LFM	8.0 ms *	7.0 kHz
LFM	8.0 ms *	13.0 kHz
LFM	8.0 ms *	22.0 kHz

- Pulse length was 8.0 ms for projectors 1,2 and 4, and 10.0 ms for projector 3.

Each signal was transmitted from a single projector at a time using a 10 Hz repetition rate for 30 s. The short CW signals were designed for estimating the time spread. Figure 3 shows 300 short CW pulses transmitted from the 67 m deep projector and received at the 217 m deep hydrophone (upper: 20 kHz; lower: 40 kHz). The received signals were match filtered to enhance signal to noise ratio. The vertical band in the left half of each panel is the Direct Path (DP) arrival; the second vertical band, about 20 msec later, is the Surface Bounce (SB) arrival.

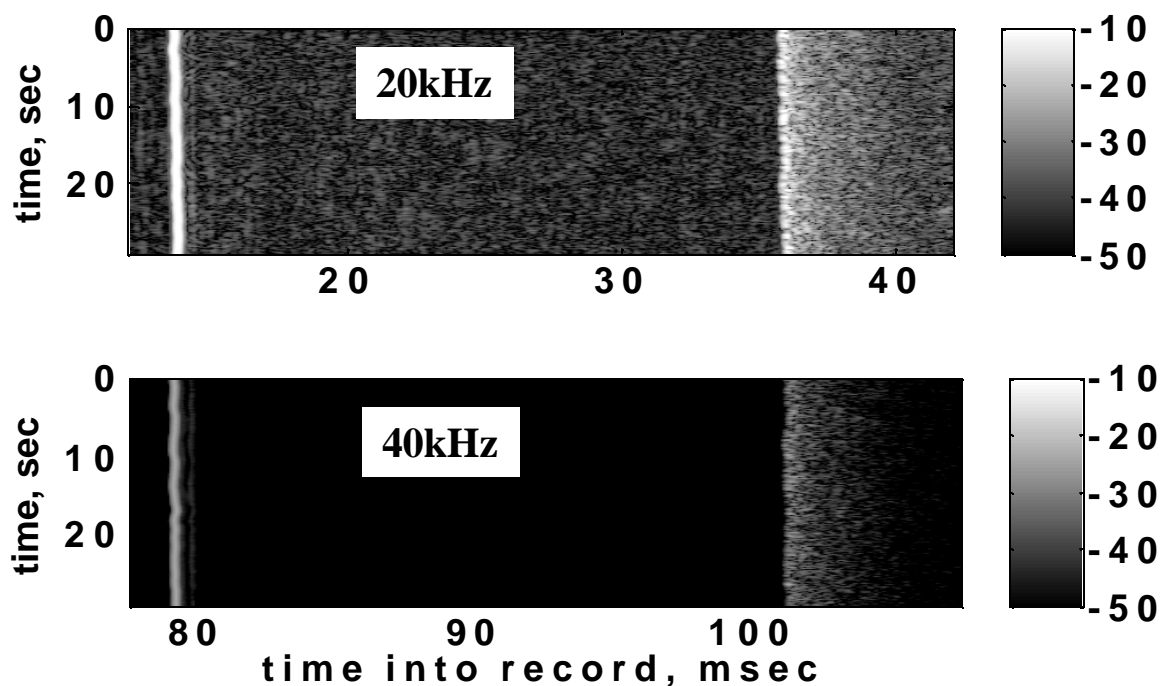


**FIGURE 3.** Acoustic data recorded at approximately 0200 UTC on 18 Aug 2002. Each panel contains a stack of ~300 short CW pulses transmitted from the 67 m deep projector and received at the 217 m deep hydrophone (upper panel: 20 kHz; lower panel: 40 kHz). Gray scale is level in dB.

Several features are evident. First, there is some jitter in the arrival times of both the DP and SB arrivals. This is due partly to relative movement between the projector and receiver but also to variation in the propagation path. Second, a fully refracted path may be seen just after the DP arrival. Third, the background level is about 10 dB lower in the 40 kHz band than in the 20 kHz band, and fourth, the DP arrival is sharp and distinct, but the SB arrival is following by a smattering of arrivals extending for 8 to 10 msec. These arrivals, which follow the SB arrival, are termed the *time spread*.

## MODEL – MEASUREMENT COMPARISON

We now extract the time spread of the surface bounce path from the data shown in Fig. 3. After aligning the SB arrivals by their leading edges, we calculate the ensemble average. The resulting time spread measurements (normalized to 0 dB peak) are solid lines in Fig. 4.

To calculate a time spread prediction, the bistatic scattering cross section model is used to calculate the intensity impulse response function  $I_{imp}(t)$ , which is then convolved with the envelope of the transmitted signal. It was important to use the receive beam pattern in this calculation. In Fig. 4, a noise floor was added to produce the time spread prediction. The agreement is good at both frequencies.

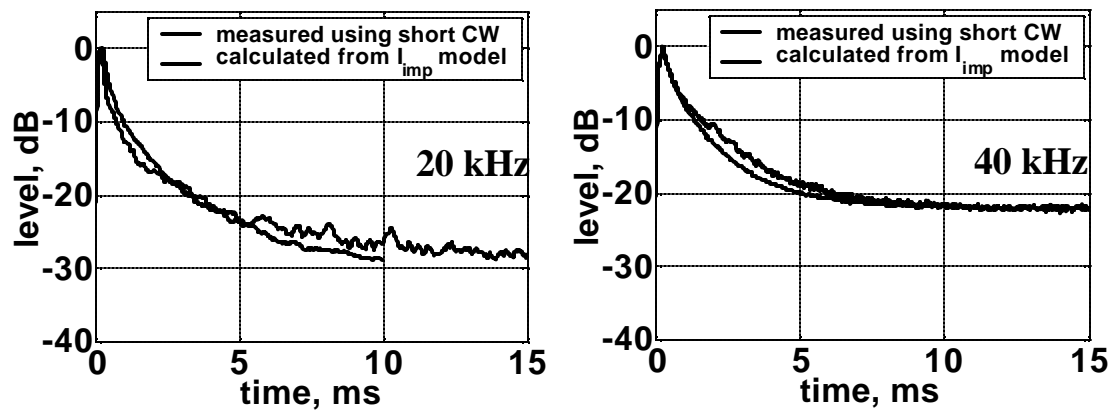


**FIGURE 4.** Time spread: measured (solid line) and predicted (dotted line) for the short CW pulses transmitted from the 67 m deep projector and received at the 217 m deep hydrophone (left: 20 kHz; right: 40 kHz). Curves are normalized to 0 dB peak.

We now compare measured frequency correlation with the theory. From the data, the frequency correlation coefficient was calculated using Equation (2), separately for the direct path and surface bounce LFM signals. A direct path arrival was used as the replica in both cases in order to account for frequency dependent absorption. The highest direct path and surface bounce path correlation coefficients were extracted from each ping and averaged over all pings to obtain an ensemble average.

The solid lines with square markers in Fig. 5 indicate the correlation coefficient of the DP arrival for the four LFM signals transmitted by the 67 m deep projector and

received at the 217 m deep receiver. The correlation of the DP arrival remains close to 1 independent of bandwidth, indicating that propagation has little effect on the correlation over all bandwidths considered. The dashed lines in Fig. 5 indicate the correlation coefficient of the SR arrival. Correlation of the SR arrival decreases with increasing bandwidth in a manner similar to that reported Keranen [15].

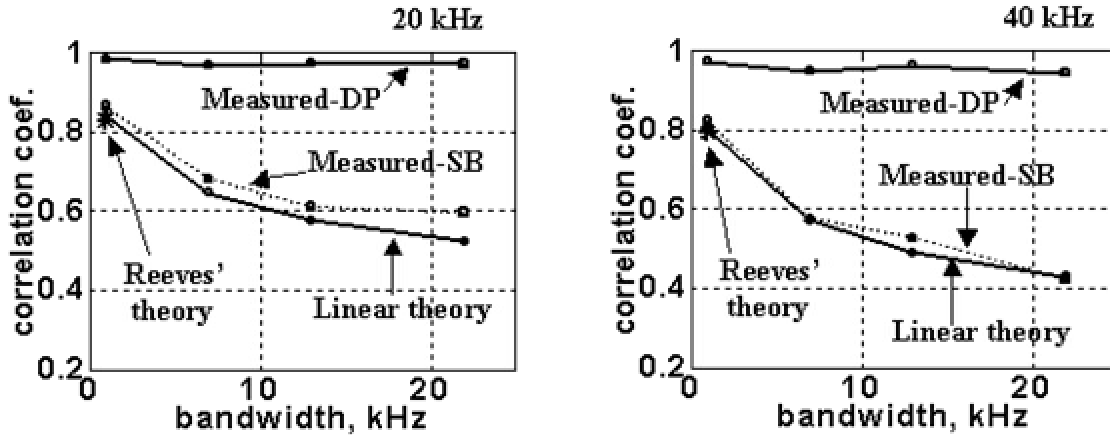


**FIGURE 5.** Frequency correlation for the 67 m deep projector and received at the 217 m deep hydrophone (left: 20 kHz; right: 40 kHz). Measured for direct path (DP) and surface bounce (SB) path; modeled using linear systems theory (circles); and modeled using Reeves' theory (asterisk).

Next we use the intensity impulse response function and apply the theory due to Reeves, calculating the ratio

$$RC_{REEVES}(b) = \frac{\int_0^T I_{imp}(t) dt}{\int_0^\infty I_{imp}(t) dt} \quad (13)$$

where the upper integration limit of the numerator is the temporal resolution of the signal. The asterisks in Fig. 5 indicate the prediction based upon Reeves' theory. That theory was developed from measurements made using signals with up to 2 kHz bandwidth, and the theory compares well with the measurements for smaller bandwidth signals.

Applying the linear systems theory, the intensity impulse response function  $I_{imp}(t)$  is Fourier transformed to obtain  $R_H(\Delta f, \Delta t)$  (Equation (11) assuming negligible frequency spread), and Equation (10) used to compute  $|\Gamma_b(\Delta f, \Delta t)|^2$  for the four LFM signals used in the measurement. Then Equation (9) is used to predict the mean replica correlation coefficient as a function of signal bandwidth. The black lines marked by circles in Fig. 5 denote the prediction based upon linear systems theory. This prediction is in good agreement with the measurements for all bandwidths, although the agreement is better at 40 kHz than at 20 kHz.

## SUMMARY AND CONCLUSIONS

We have presented ocean surface forward scatter time spread and frequency correlation measurements made in August 2002, about 2500 m east of San Clemente Island, California, under very modest sea states. Our time spread measurements were found to compare well with predictions calculated using a bistatic scattering cross section model developed by Peter Dahl [8-10]. Our frequency correlation measurements were compared with two different theories. The first is a physics-based theory published by Jon Reeves nearly 30 years ago [5]. Consistent with his own measurements, Reeves' theory is found to match our measured correlation well for signal bandwidths up to 2 kHz. Second, we used linear systems theory [11] to develop the equations connecting frequency correlation and time spread. We find that frequency correlation predicted using the linear systems theory matches measured correlation very well. An important next step in this work is to validate the linear systems theory for higher sea state conditions.

## ACKNOWLEDGMENTS

This work was supported by the Office of Naval Research (Dr. J. Tague, Code 321US) under award No. N00014-02-1-0156. The measurement involved significant cooperation from the many people at the Marine Physical Laboratory (MPL) of Scripps Institution of Oceanography, especially Capt. Bill Gaines (USN-Ret) and Dr. Gerald D'Spain. Acoustics graduate students Steven Lutz, Rachel Romond and Tom Weber did superb work at sea and their contributions are appreciated.

## REFERENCES

1. Fortuin, L., J. Acoust. Soc. Am **47**, 1209- 1228 (1969).
2. Ogilvy, J.A., *Theory of Wave Scattering from Random Rough Surfaces*, Bristol, England: Institute of Acoustics, 1991.
3. Dahl, P.H., J. Acoust. Soc. Am. **115**, 589-599 (2004).
4. Bendat, J.S. and A.G. Piersol, *Random Data: Analysis and Measurement Procedures, 2<sup>nd</sup> Ed.*, New York: John Wiley and Sons, 1986.
5. Reeves, J.C., *Distortion of Acoustic Pulses Reflected from the Sea Surface*, Ph.D. Dissertation, University of California, Los Angeles (1974).
6. Martin, J.J., J. Acoust. Soc. Am **43**, 405-417 (1968).
7. Weston, D.E., J. Acoust. Soc. Am. **37**, 119-124 (1965).
8. Dahl, P.H., J. Acoust. Soc. Am. **100**, 748-757 (1996).
9. Dahl, P.H., J. Acoust. Soc. Am. **105**, 2155-2169 (1999).
10. Dahl, P.H., IEEE J. Oceanic Eng. **26**, 141-151 (2001).
11. Ziomek, L.J., *Underwater Acoustics: A Linear Systems Theory Approach*, Orlando: Academic Press, 1985.
12. Weinberg, H. and R.E. Keenan, NUWC-Newport TR 10,568, Naval Undersea Warfare Center Division Newport, Rhode Island, 1996.
13. Groves, D.G. and L.M. Hurt, *Ocean World Encyclopedia*, New York: McGraw-Hill, 1980.
14. Plant, W.J., J. Geophys. Res. **107(C9)**, 3120, doi:10.1029/2001JC000909, 2002.
15. Keranen, J.G., *Effect of the Ocean Environment on the Coherence of Broadband Signals*, MS Thesis, The Pennsylvania State University, State College, PA (2001).